CREEP CAVITATION IN SILICON NITRIDE BY PULSE-ECHO TECHNIQUE

FRANTIŠEK LOFAJ[1]

The pulse-echo technique for ultrasonic velocity measurement was used for nondestructive study of creep damage in an advanced silicon nitride, SN 88, during interrupted tensile creep tests at 1400 °C under stress of 150 MPa. Linear relationships were found between strain and the longitudinal and shear wave velocities, Poisson's ratio, Young's, shear and bulk moduli. Density measurement indicated a coefficient of proportionality of ~ 0.7 between the volume fraction of cavities and tensile strain. Cavitation was therefore concluded to be the main creep mechanism and the reason for ultrasonic velocity and elastic moduli degradation in the studied silicon nitride. The ultrasonic velocity technique was demonstrated to be simple, sensitive and reliable nondestructive method for monitoring of creep damage during intermittent creep in silicon nitride.

K e y w o r d s: tensile creep, cavitation, ultrasonic velocity, silicon nitride, elastic moduli

KVANTIFIKÁCIA CREEPOVEJ KAVITÁCIE V NITRIDE KREMÍKA ULTRAZVUKOVOU METÓDOU SIGNÁL-ODRAZ

V práci bola na nedeštruktívnu kvantifikáciu creepového poškodenia počas prerušovanej ťahovej deformácie pri 1400 °C a napätí 150 MPa v komerčnom nitride kremíka SN 88 použitá metóda signál-odraz na meranie rýchlosti zvuku. Pomocou danej metódy sa našli lineárne závislosti rýchlosti pozdĺžnych a priečnych vĺn, Poissonovho pomeru, Youngovho, šmykového a objemového modulu od veľkosti deformácie. Merania hustoty tiež ukázali, že zmena hustoty, ktorá zodpovedá objemovému podielu kavít, závisí lineárne od deformácie so smernicou ~ 0.7. Z toho vyplýva, že kavitácia je v danom materiáli hlavným creepovým mechanizmom a príčinou degradácie rýchlosti zvuku a modulov pružnosti. Meranie rýchlosti zvuku je jednoduchá, dostatočne citlivá a spoľahlivá metóda na nedeštruktívnu kontrolu creepového poškodenia v nitride kremíka počas prerušovaného creepu.

1. Introduction

The design of ceramic components from silicon nitride and other ceramics requires detail understanding of the processes during creep deformation, especially

[1] Institute of Materials Research of the Slovak Academy of Sciences, 043 53 Košice, Slovak Republic, e-mail: lofaj@saske.sk

those controlling lifetime. In the case of structural components, which are subjected to high loads at elevated temperatures for prolonged period of time, creep is the principal limitation. Numerous creep studies found that cavitation plays an important role in tensile deformation in silicon nitride [1–10]. Cavities contribute to deformation since their volume is transformed into tensile strain. The relationship between tensile strain and relative density change, which is equal to the volume fraction of cavities, is linear with a slope close to 1.0 for a wide range of ceramics. Therefore, cavitation was concluded to be the main creep mechanism in silicon nitride and other vitreous bonded ceramics [4–10].

Cavitation can be studied by various methods. The simplest method, density measurement, provides information only on the total volume of cavities. Transmission electron microscopy yields only qualitative information about the individual cavities. Note that these methods are destructive and cannot be used for the monitoring of cavity accumulation in structural components, e.g. in ceramic blades during periodic overhauls. Pulse-echo transit-time technique is a non-destructive method for the measurement of the ultrasonic velocity, which is often used for the quality control of metals, glasses and ceramics with different levels of porosity [11–25]. However, earlier experiments were generally carried out on highly porous materials to investigate the relationship between porosity and elastic moduli. They were not used for the study of microstructural changes during deformation. Limited number of preliminary studies on silicon nitride after creep deformation showed that the technique can also detect cavitation related density changes [23–25]. The changes in the ultrasonic velocity of the longitudinal and shear waves, v_l and v_t, respectively, calculated from the measured transit time, allow us to determine also the corresponding Poisson's ratio, ν, Young's modulus, E, shear modulus, G, and bulk modulus, K, according to the well known relationships [11–12]

$$\nu = [1 - 2(v_\mathrm{t}/v_\mathrm{l})^2]/[2 - 2(v_\mathrm{t}/v_\mathrm{l})^2], \tag{1}$$

$$E = v_\mathrm{l}^2 \rho(1 + \nu)(1 - 2\nu)/(1 - \nu), \tag{2}$$

$$G = v_\mathrm{t}^2 \rho, \tag{3}$$

$$K = E/3(1 - 2\nu), \tag{4}$$

where ρ is the density of the material. Thus, the pulse-echo technique has a potential for monitoring cavity accumulation and related elastic moduli change during creep, as well. However, the number of tests in those studies was rather limited and the scatter of the Young's modulus data reduced the accuracy of the coefficient between strain and cavitation [23].

The objective of the current work is to investigate the potential of the pulse-echo technique for non-destructive quantification of cavitation during intermittent tensile creep in an advanced silicon nitride.

2. Experimental procedure

Tensile creep

The study was carried out on a commercial silicon nitride grade material designated SN 88 (NGK Insulators, Ltd., Nagoya, Japan). Material composition and mechanical properties of this silicon nitride grade were described elsewhere [8, 26]. Tensile creep tests were performed on eleven pin-loaded tensile creep specimens of total length 76 mm (type SR 76 [27]). Their gauge size was $2.5 \times 2.5 \times 19$ mm. Tensile stresses were applied using single-pin SiC pull rods and a pneumatic loading system. Creep strain was measured by scanning laser extensometry and two SiC flags attached to the gauge of the specimen [28].

Two types of creep experiments were conducted in the same creep machine at 1400 ℃ in air and under a tensile stress of 150 MPa. The first set of creep experiments included nine specimens. Eight tests were intentionally interrupted at various strain levels prior to failure. The ninth test lasted until rupture without any interruption. Then, samples for sound velocity and density measurements were cut from these specimens. The second type of creep experiments was carried out on two samples conditionally designated as A and B. These tests were periodically interrupted after predetermined increments of strain and the specimens cooled down under load. The samples were reloaded into the creep machine after making ultrasonic velocity measurements, and deformed for another increment of strain. This procedure was repeated six times for both samples.

Ultrasonic velocity measurement

The pulse-echo technique involves a time-of-flight measurement to determine the ultrasonic velocity [11–12]. Piezoelectric transducers operating at 20 MHz and 10 MHz, driven by shock excitation using a pulser/receiver with a bandwidth of 200 MHz (Model 5900 PR, Panametrics, USA), were used to generate the longitudinal and transverse waves, respectively. Silicone oil and a multipurpose, water soluble, high viscosity liquid were used as the ultrasonic couplants between the specimens and the corresponding transducer delay rod.

The transit time, τ_x, ($x = l$ for longitudinal waves and $x = t$ for transverse or shear waves) for a sample round trip was measured between multiple echoes using a digital oscilloscope. Measurements were made in the gauge zone in three different locations and in two transverse directions both across the width and across the thickness of the gauge (perpendicular to the tensile stress). The intervals in the grips were measured at four locations in one direction. The specimen thickness, d, was determined using a digital micrometer with an accuracy of ± 2 μm. Ultrasonic velocity of the corresponding waves was calculated from $v_x = 2d/\tau_x$.

The measurements on specimens A and B were performed on the samples with the oxide layers. Nine specimens from a second set of creep experiments were cut

and the samples from the gauge and grip areas were ground to remove the oxide layers. They were subsequently used for density and sound velocity measurements.

The relative sound velocity change was determined as a difference between the velocities in the gauge and the corresponding velocity in an undeformed grip, v_{x0}, from

$$\Delta v_x/v_{x0} = (v_x - v_{x0})/v_{x0}. \tag{5}$$

Density measurement

The sink-float technique was used for the measurement of specimen density [4]. Bars with dimensions of $2.3 \times 1.7 \times 10$ mm were cut from the gauge and grip regions of nine specimens following creep tests. They were placed in a water solution of thallium malonate formate in a borosilicate glass-jacketed tube connected to the constant temperature water recirculator. The solution density was adjusted by adding a small amount of distilled water at room temperature until the heaviest specimen started to sink. The temperature coefficient of the density solution was calibrated using two floats of known density (R.P. Cargille Laboratories, Cedar Groove, NJ) certified to ± 0.0005 g/cm^3. By adjusting the temperature of the solution with the water recirculator, it was possible to bracket the buoyancy temperature of each specimen with an accuracy better than 0.5 ℃. Knowing the temperature coefficient of the solution density change, the density of the specimens was calculated from the measured buoyancy temperature. The relative density change, which is equivalent to the volume fraction of cavities, f_v, was determined from the difference between the deformed gauge sample density, ρ_gauge, and the undeformed grip sample density, ρ_grip,

$$f_\mathrm{v} = \Delta\rho/\rho_\mathrm{grip} = (\rho_\mathrm{grip} - \rho_\mathrm{gauge})/\rho_\mathrm{grip}. \tag{6}$$

TEM study

The samples for the transmission electron microscopy (TEM) studies were cut parallel to the direction of the applied stress from the gauge specimens used for ultrasonic and density measurements. The foils were prepared according standard procedure involving four-step hand grinding and polishing, dimpling, and ion milling. Transmission electron microscopy investigations on carbon coated specimens at 200 kV (EM 300, Philips, The Netherlands) were carried out to confirm the presence and to investigate the type of cavities formed during creep.

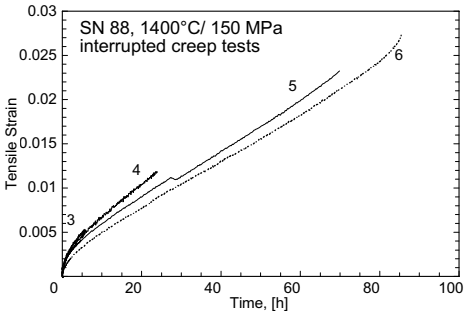

Fig. 1. Tensile creep curves from the interrupted creep tests in SN 88 at 1400 °C under stress of 150 MPa. The sample No. 3 was tested for 5.7 h up to a strain of $\varepsilon = 0.51$ %, No. 4 for 24 h and $\varepsilon = 1.20$ %, No. 5 for 70 h and $\varepsilon = 2.30$ % and No. 6 failed after 85.06 h at the failure strain of 2.70 %.

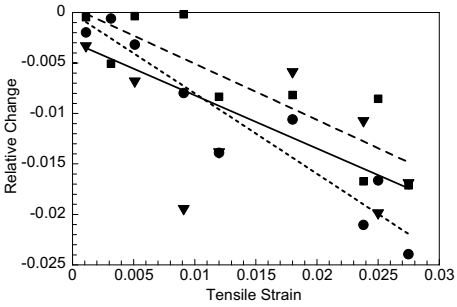

Fig. 2. Strain dependence of the relative change of the ultrasonic velocities for longitudinal waves, shear waves and Poisson's ratio for nine interrupted creep tests (● – longitudinal wave velocity, ■ – shear wave velocity, ♦ – Poisson's ratio).

Table 1. Strain and porosity dependences of the elastic moduli in silicon nitride deformed at 1400 °C under a stress of 150 MPa from ultrasonic velocity and density measurements

Elastic moduli dependence	Coefficients of strain dependence	Coefficients of porosity dependence	Literature data
$\Delta E/E_0$	$k_E = 1.\ 94$ ($R = 0.9682$)	$b_E = 2.73$ ($R = 0.9518$)	1.74 [16], 3.11[A] [16], 2.39/2.32[B] [16], 2.36/2.82[C] [16], 2.00–3.03 [17], 2.44 [23]
$\Delta G/G_0$	$k_G = 1.78$ ($R = 0.9448$)	$b_G = 2.49$ ($R = 0.9242$)	2.27 [16] 2.0 [19]
$\Delta K/K_0$	$k_K = 2.52$ ($R = 0.9545$)	$b_K = 3.\ 61$ ($R = 0.9583$)	–
$\Delta\rho/\rho_0$	$k_\rho = 0.69$ ($R = 0.9928$)	1.0 –	0.75 [25], 0.90 [8–9], 0.93±0.04 [4], 0.8–1.0 [6, 10], 1.02±0.03 [29]

[A] – $Y_2O_3 + SiO_2$ doped silicon nitride, porosity range $P < 12$ %; [B] – CeO_2 doped silicon nitride, $P < 38$ % and $P < 13$ %, respectively; [C] – MgO-doped silicon nitride, porosity range up to 44 % and 13 %, respectively.

3. Results

Fig. 1 illustrates several creep curves obtained from the interrupted creep tests at 1400 °C. Three tests were interrupted during primary stage of creep, fourth and fifth tests during steady state-like stage, and the last test (No. 6) ran until failure.

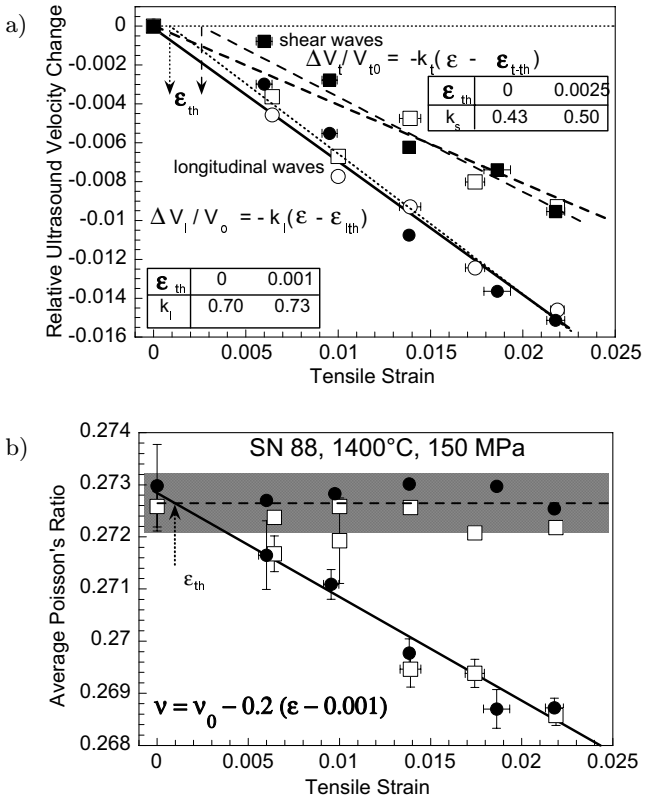

Fig. 3. Strain dependence of the relative change of the ultrasonic velocities for longitudinal waves and shear waves – a), of the absolute values of Poisson's ratio – b) in samples A (open symbols) and B (full symbols).

Fig. 2 shows relative changes of the longitudinal and shear wave velocities and that of the Poisson's ratio in the gauge sections of these samples, whereas Figs. 3a,b illustrate similar dependences in the second set of experiments (A and B). The absolute values of mean velocities of the longitudinal and shear waves in the grips were approximately constant and in the range of 10 390 ± 35 m/s and 5 815 ± 20 m/s, respectively, regardless of the annealing time, while the velocities in the gauges decreased with strain. The relative velocities from samples A and B can be linearly fit with high confidence – regression coefficients R in the case of longitudinal waves are $R = 0.995$ and 0.996, respectively, and the slopes are 0.67 and 0.86. The scatter in the case of relative shear waves is slightly higher ($R = 0.936$ and 0.987 for samples A and B, respectively) and the corresponding slopes are 0.50 and 0.40. The slopes

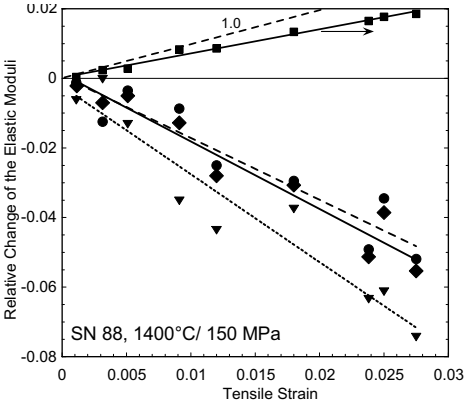

Fig. 4. Tensile strain vs. relative density change (■ symbols), relative Young's (⧫), shear (●) and bulk (▼) moduli. The slope coefficients are summarized in Table 1.

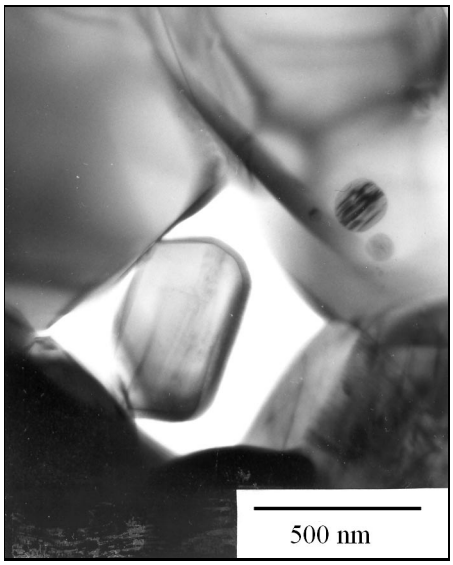

Fig. 5. TEM micrograph of the microstructure after creep shows the presence of the multigrain junction cavities.

of the strain dependence for nine different ground gauges are 0.79 ($R = 0.948$) for longitudinal waves and 0.56 ($R = 0.859$) for shear waves. Large scatter in this set is possibly due to material differences amongst different batches. In the case of Poisson's ratio, the slope of its linear dependence on strain was approximately -0.53 ($R = 0.626$). Mean value of the Poisson's ratio was 0.2727 ± 0.0015 (Fig. 3b).

Fig. 4 combines the strain dependence of the relative density change and elastic moduli. The density data fit a linear relationship over the whole strain range investigated, with a coefficient of proportionality of 0.69 and $R = 0.993$. Elastic moduli were calculated according to Eqs. (2) to (5). The elastic modulus values in the grips were 304.3 ± 1.5 GPa for Young's modulus, 119.6 ± 0.7 GPa for the shear modulus, and 223.0 ± 1.6 GPa for the bulk modulus, and they decreased approximately linearly with strain. Note that the test data terminated prior to failure fall on the same line as the data taken on the samples strained to failure at 2.75 %. The values of the slopes of linear fits between strain and elastic moduli are summarized in Table 1.

The results of TEM study are illustrated in Fig. 5. Relatively many multigrain junction cavities were found in the gauge zone after deformation at 1400 ℃. Other

types of cavities, reported earlier for similar grade of silicon nitride after long-term creep tests [26] were not detected.

4. Discussion

The repeated ultrasonic velocity measurements on samples A and B indicate that the effect of deformation can be distinguished from the scatter of the undeformed material at strains greater than 0.3 % (Fig. 1). The detection limit of the technique on other samples is reduced to around 0.5 % or greater due to larger scatter. This is possibly due to variations in the initial porosity between specimens made from different batches. The effect of the oxide layers is negligible: The longitudinal wave velocities in the samples with an oxide layer differ only marginally from the fitted velocities in the ground samples. The slopes of the linear fits are also very similar (Table 1). The velocity of shear waves is approximately one-half as great and, therefore, the relative scatter is larger (Fig. 2). Slopes of the fitted dependences vary more than in the case of longitudinal waves. Thus, shear waves are less effective for detecting the changes. However, the combination of both velocities in calculating Poisson's ratio eliminated the variations, and the results from both sets of data were nearly identical. Consequently, the pulse-echo technique using longitudinal waves is preferable for the reliable detection of changes in the microstructure of silicon nitride during deformation at strains above ~ 0.3 %. Measurements can be performed without removing the thin oxide layers from material surfaces, which is very important for repeated non-destructive monitoring of structural components.

Elastic moduli calculations require precise sample velocity and density measurements. The non-destructive character of the pulse echo technique is lost at this stage since oxide layers should have to be ground away. However, as will be shown later, the absolute values of elastic moduli are not necessary for monitoring purposes, especially, when the physical reasons for ultrasonic velocity changes and elastic moduli degradation are better understood.

Young's, shear and bulk moduli degrade during deformation. It is noteworthy that all the parameters measured or calculated (ultrasonic velocities, density and elastic moduli) decrease linearly with strain. The coefficients of proportionality are around 2.0 for both Young's and shear moduli, and approximately 2.3 for the bulk modulus. It is noted that a comparison of the coefficients of proportionality with the literature data for silicon nitride [16–17, 19–22] is not possible because elastic moduli were usually investigated for their dependence on porosity, not on strain.

Fig. 4 indicates that deformation generates density changes, which are equivalent to the introduction of additional porosity. The only possible explanation for the increase of creep related porosity, besides growth of internal cracks, is the accumulation of cavities as confirmed by TEM observation (Fig. 5). Several earlier electron microscopy studies also demonstrated that the most common type of cavities in

SN 88 are multigrain junction cavities [5–9]. Thus, density changes in Fig. 4 unambiguously result from cavitation. The relationship between the volume fraction of cavities and tensile strain, ε, is [8, 24–25]

$$f_{\mathrm{v}} = k_{\rho}(\varepsilon - \varepsilon_{\mathrm{th}}), \tag{7}$$

where k_{ρ} is the coefficient of proportionality and $\varepsilon_{\mathrm{th}}$ is a threshold strain for cavitation. The physical meaning of this dependence is that cavities accumulate continuously starting from a small threshold strain (the x-axis intercept is close to zero), and about 69 % of the strain results from cavitation. Although the coefficient of proportionality of 0.69 is less than the value of ~ 0.9 reported earlier for the same material [6, 8, 10], cavitation remains the dominant creep mechanism.

The relationship (7) allows us to transform the dependences between elastic moduli and strain to relationships between elastic moduli and porosity (volume fraction of cavities). Young's modulus degradation with porosity has been described by a variety of equations [13–25]. However, for small porosity values, all relationships simplify to the first order as:

$$E/E_0 = 1 - b_{\mathrm{E}}p, \tag{8}$$

where E_0 is the Young's modulus of a pore-free material, the porosity p equals the volume fraction of cavities, f_{V}, and b_{E} is the coefficient of proportionality. The elastic moduli from Fig. 4 linearly decrease also in dependence on porosity related to cavitation. The corresponding coefficients of proportionality for various elastic moduli are shown in Table 1.

Numerous studies of the porosity dependence for the elastic moduli of highly porous materials indicate that a non-linear relationship can be expected to fit the experimental data better than may a linear relationship [16–18]. However, the linear dependence in Eq. (8) is appropriate for the small porosities as a first order approximation. Table 1 contains also linear coefficients reported by various authors for Young's modulus degradation in porous silicon nitrides. Phani [16] reported $b_{\mathrm{E}} = 1.74$ for sintered silicon nitrides with a porosity range of 0 to 26 %. His analysis of the literature showed values for b_{E} to lie in the range of 2.3 to 2.8, depending on porosity and sintering additives in various silicon nitride grades. Datta et al. [17] analyzed extensive data sets and found coefficients in the range of 2.00 to 3.03 for porosities up to 38 %. Cao et al. [23] found a coefficient of 2.44 in SN 88M. Fate [19] obtained a value of b_{G} close to 2.0, whereas 2.27 was reported by Phani [16]. All these coefficients agree reasonably well with those measured in the current study involving considerably smaller strains. This provides additional confirmation that cavitation is the main creep mechanism in vitreous bonded silicon nitride ceramics.

From the practical point of view, the measurement of ultrasonic velocity changes is sufficient for monitoring cavity accumulation due to the unambiguous correlation between damage accumulation and ultrasonic velocity change. Destructive and time-consuming density measurement can be avoided.

5. Conclusions

The pulse-echo ultrasonic velocity technique revealed linear relationships between tensile strains, ultrasonic velocity and elastic modulus degradation for strains up to 3 %. Cavity accumulation was identified as the main reason for a decrease of the ultrasonic velocity and a degradation of the elastic moduli. Cavitation was confirmed to be the main creep mechanism in the silicon nitride materials studied. The measurement of the change in velocity of the longitudinal ultrasonic waves is preferred and sufficient for the quantification of cavitation during creep. The capability of the ultrasonic velocity technique for simple, highly sensitive and reliable nondestructive monitoring of creep damage in silicon nitride ceramics has been demonstrated.

Acknowledgements

The support of the Fulbright Commission and of NIST for F. Lofaj's stay at NIST is gratefully acknowledged. The work was partially supported by the VEGA (Slovakia) Project No. 2/7011/21. The contributions of Gerry V. Blessing, W. E. Luecke and S. M. Wiederhorn (NIST) to this work are highly appreciated.

REFERENCES

[1] MENNON, M. N.—FANG, H. T.—WU, D. C.—JENKINS, M. G.—FERBER, M. K.—MOORE, K. L.—HUBBARD, C. R.—NOLAN, T. A.: J. Am. Ceram. Soc., *77,* 1994, p. 1217.
[2] FERBER, M. K.—JENKINS, M. G.—NOLAN, T. A.—YECKLEY, R. L.: J. Am. Ceram. Soc., *77,* 1994, p. 657.
[3] GASDASKA, C. J.: J. Am. Ceram. Soc., *77,* 1994, p. 2408.
[4] LUECKE, W. E.—WIEDERHORN, S. M.—HOCKEY, B. J.—KRAUSE jr., R. E.—LONG, G. G.: J. Am. Ceram. Soc., *78,* 1995, p. 2085.
[5] LOFAJ, F.—CAO, J. W.—OKADA, A.—KAWAMOTO, H.: In: Proc. 6th Int. Symp. Ceramic Materials & Components for Engines. Tokyo, Technoplaza Co., Inc. 1997, p. 713.
[6] LUECKE, W. E.—WIEDERHORN, S. M.: J. Am. Ceram. Soc., *82,* 1999, p. 2769.
[7] KRAUSE jr., R. E.—LUECKE, W. E.—FRENCH, J. D.—HOCKEY, B. J.—WIEDERHORN, S. M.: J. Am. Ceram. Soc., *82,* 1999, p. 1233.
[8] LOFAJ, F.: Mater. Sci. Eng. A, *279,* 2000, p. 61.
[9] LOFAJ, F.—OKADA, A.—KAWAMOTO, H.: J. Am. Ceram. Soc., *80,* 1997, p. 1619.
[10] WIEDERHORN, S. M.—HOCKEY, B. J.—LUECKE, W. E.: J. Eur. Ceram. Soc., *19,* 1999, p. 2273.
[11] ASTM E 494-95, Standard Practice for Measuring Ultrasonic Velocity in Materials. Vol. 03.03, 1999. Annual Book of ASTM Standards. Philadelphia, ASTM 1999, p. 185.

[12] BLESSING, G. V.: In: ASTM STP 1045, Dynamic Elastic Modulus Measurements in Materials. Philadelphia, ASTM 1990, p. 47.
[13] HASHIN, Z.: J. Appl. Mech., Trans. ASME, *29,* 1962, p. 143.
[14] SPRIGGS, R. M.: J. Am. Ceram. Soc., *44,* 1961, p. 628.
[15] DEAN, E. A.—LOPEZ, J. A.: J. Am. Ceram. Soc., *66,* 1983, p. 366.
[16] PHANI, K. K.—NIYOGI, S. K.: J. Mater. Sci. Lett., *6,* 1987, p. 511.
[17] DATTA, S. K.—MUKHOPADHYAY, A. K.—CHAKRABORTY, D.: Am. Ceram. Soc. Bull., *68,* 1989, p. 2098.
[18] KUPKOVA, M.: J. Mater. Sci., *28,* 1993, p. 5265.
[19] FATE, W. A.: J. Am. Ceram. Soc., *57,* 1974, p. 372.
[20] THORP, J. S.—BUSHELL, T. G.: J. Mater. Sci., *20,* 1985, p. 2265.
[21] ROTH, D. J.—STANG, D. B.—SWICKARD, S. M.—DEGUIRE, M. R.—DOLHERT, L. E.: Materials Eval., *49,* 1990, p. 883.
[22] PANAKKAL, J. P.: Materials Eval., *56,* 1997, p. 1367.
[23] CAO, J.—W.—LOFAJ, F.—OKADA, A.: J. Mat. Sci., *36,* 2001, p. 1301.
[24] LOFAJ, F.—BLESSING, G. V.—WIEDERHORN, S. M.: J. Am. Ceram. Soc., to be published.
[25] LOFAJ, F.—SMITH, D. T.—BLESSING, G. V.—LUECKE, W. E.—WIEDERHORN, S. M.: J. Mater. Sci., in preparation.
[26] LOFAJ, F.—USAMI, H.—OKADA, A.—KAWAMOTO, H.: J. Am. Ceram. Soc., *82,* 1999, p. 1009.
[27] FRENCH, J. D.—WIEDERHORN, S. M.: J. Am. Ceram. Soc., *79,* 1996, p. 550.
[28] LUECKE, W. E.—FRENCH, J. D.: J. Am. Ceram. Soc., *79,* 1996, p. 16.

Received: 14.1.2002